Journal of Alloys and Compounds 509 (2011) 7105–7108

Contents lists available at ScienceDirect

Journal of Alloys and Compounds

journal homepage: www.elsevier.com/locate/jallcom

Polarization-dependent electrolyte electroreflectance study of Cu_2ZnSiS_4 and $Cu_2ZnSiSe_4$ single crystals

S. Levcenco[a,1], D. Dumcenco[a,1], Y.S. Huang[a,*], E. Arushanov[b], V. Tezlevan[b], K.K. Tiong[c], C.H. Du[d]

[a] Department of Electronic Engineering, National Taiwan University of Science and Technology, Taipei 106, Taiwan
[b] Institute of Applied Physics, Academy of Sciences of Moldova, Chisinau, MD 2028, Republic of Moldova
[c] Department of Electrical Engineering, National Taiwan Ocean University, Keelung 202, Taiwan
[d] Department of Physics, Tamkang University, Tamsui 251, Taiwan

ARTICLE INFO

Article history:
Received 15 February 2011
Accepted 3 April 2011
Available online 9 April 2011

PACS:
71.35.Cc
78.40.−q
78.40.Fy

Keywords:
Semiconductors
Optical properties
Optical spectroscopy

ABSTRACT

Polarization-dependent electrolyte electroreflectance (EER) measurements were carried out on the oriented Cu_2ZnSiS_4 and $Cu_2ZnSiSe_4$ single crystals at room temperature. Thin blade single crystals of Cu_2ZnSiS_4 and $Cu_2ZnSiSe_4$ were grown by chemical vapor transport technique using iodine as a transport agent. Laue pattern normal to the basal plane of the as-grown crystal revealed the formation of orthorhombic structure with the normal along [2 1 0] and the **c** axis parallel to the long edge of the crystal platelet. The polarized EER spectra in the vicinity of the direct band edge of Cu_2ZnSiS_4 displayed distinct structures associated with transitions from two upper-most valence bands to the conduction band minimum at Γ point. In the $\mathbf{E}\perp\mathbf{c}$ configuration, the feature designated as $E_A \sim 3.345$ eV was detected and for $\mathbf{E}\parallel\mathbf{c}$, only $E_B \sim 3.432$ eV appeared. For $Cu_2ZnSiSe_4$, three features denoted as E_A, E_B, and E_C at around 2.348, 2.406 and 2.605 eV, respectively, were recorded for $\mathbf{E}\perp\mathbf{c}$ polarization, whereas in the $\mathbf{E}\parallel\mathbf{c}$, only E_B and E_C were the allowed transitions. Based on the experimental observations and a recent band-structure calculation by Chen et al. [Phys. Rev. B 82 (2010) 195203], plausible band structures near the direct band edge of Cu_2ZnSiS_4 and $Cu_2ZnSiSe_4$ have been proposed.

1. Introduction

Cu_2ZnSiS_4 and $Cu_2ZnSiSe_4$ belong to the family of quaternary chalcogenide crystallizing in the wurtzite–stannite structure. In these compounds each sulfur/selenium atom has four nearest neighbor cation atoms (two copper atoms, a zinc, and a silicon atom) at the corners of the surrounding tetrahedron [1–4]. The quaternary chalcogenide semiconductors have drawn wide interest for their nonlinear optical properties [5,6] and potential application as solar-cell absorbers [7–9], photocatalysts for solar water splitting [10,11], and high-temperature thermoelectric materials [12,13]. Despite their interesting optical and thermoelectric properties, and possible applications, up-to-date, only a few studies have been reported concerning the basic properties of $Cu_2ZnSiS_4(Se_4)$, due to the difficulty of preparing suitable size, compositionally homogeneous and high purity single crystals. Furthermore, the reported results of these studies [14,15] contain some discrepancies.

In this article, we report a detailed study of the near direct band edge anisotropic optical transition properties of Cu_2ZnSiS_4 and $Cu_2ZnSiSe_4$ single crystals by polarization-dependent electrolyte electroreflectance (EER) at room temperature. High quality single crystals of Cu_2ZnSiS_4 and $Cu_2ZnSiSe_4$ were grown by chemical vapor transport using iodine as the transport agent. Hall measurements indicated p-type semiconducting behavior for the crystals. The EER measurements were carried out on the as-grown basal plane with the normal along [2 1 0] and the axis **c** parallel to the long edge of the crystal platelets. The polarization-dependent near band-edge excitonic transition energies were determined. Base on a recent band-structure calculation by Chen et al. [16,17], a schematic representation of the plausible assignments for the observed near direct band edge optical transitions for Cu_2ZnSiS_4 and $Cu_2ZnSiSe_4$ is presented and discussed.

2. Experimental

Single crystals of Cu_2ZnSiS_4 ($Cu_2ZnSiSe_4$) were grown by vapor transport of stoichiometric amounts of the elements with 5 mg iodine/cm^3 as the transport agent. Optimum crystal growth was achieved with the charge zone maintained at 950 °C (850 °C) and the growth zone at 900 °C (800 °C). The transport process was carried out for a period of 14 days. Single crystals Cu_2ZnSiS_4 ($Cu_2ZnSiSe_4$) formed thin, greenish (reddish), blade shape up to 10 mm × 1.5 mm (20 mm × 1.0 mm) in area

* Corresponding author. Tel.: +886 2 27376385; fax: +886 2 27376424.
E-mail address: ysh@mail.ntust.edu.tw (Y.S. Huang).
[1] Permanent address: Institute of Applied Physics, Academy of Sciences of Moldova, Chisinau, MD 2028, Moldova.

0925-8388/$ – see front matter © 2011 Elsevier B.V. All rights reserved.
doi:10.1016/j.jallcom.2011.04.013

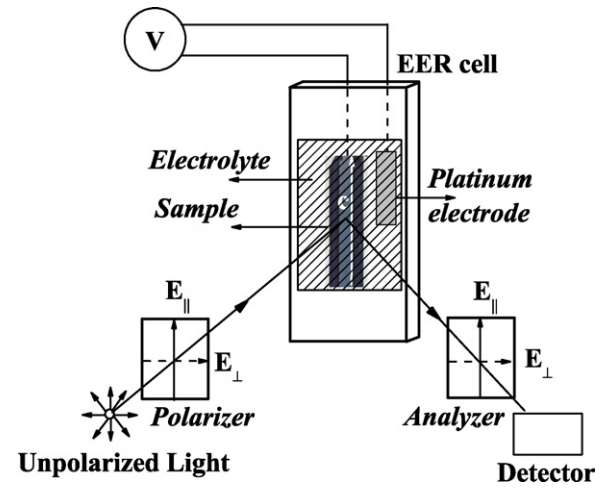

Fig. 1. A schematic arrangement of the polarization-dependent EER measurements.

and 300 (100) μm in thickness were synthesized. Hall measurements indicated p-type semiconducting behavior for the as-grown crystals. The orientation of the basal plane was determined by comparing back-reflection Laue pattern with computer generated Laue plots. Analyzing the symmetry of Laue pattern confirms the formation of orthorhombic structure and reveal that the normal of the basal plane is [2 1 0] and the long-edge of the crystal platelet is parallel to **c** axis [18].

Fig. 1 depicts the schematic arrangement of the polarization-dependent EER measurements with polarization configurations of **E**⊥**c** and **E**∥**c** performed on the as-grown basal plane with the normal along [2 1 0] and **c** parallel to the long edge of the crystal platelet. A 150W xenon arc lamp filtered by a 0.25 m grating monochromator provided the source for EER measurements. Model PRH 8020 CASIX Rochon prisms were employed for polarization dependent measurements. A model 3378 Hamamatsu photomultiplier tube was used to detect the reflected signal. For EER measurements an electrolyte of the tartaric acid (3 wt.%) in ethylene alcohol was used. A 200 Hz, 4 V peak-to-peak, square wave with a −0.5 V (vs. Pt electrode) DC bias was used to modulate the electric field. A dual-phase lock-in amplifier was used to measure the detected signals. The entire data acquisition procedure was performed under computer control. Multiple scans over a given photon energy range was programmed until a desired signal-to-noise level has been obtained.

3. Results and discussion

Fig. 2(a)–(c) shows the unpolarized, **E**⊥**c** and **E**∥**c** polarization EER spectra of Cu_2ZnSiS_4 in the energy range 3.2–3.6 eV, respectively. As shown in Fig. 2(a), the unpolarized EER spectrum has two prominent features labeled as E_A and E_B and located between 3.20 and 3.55 eV. The polarized spectra showed evidence of the existence of a strong polarization effect on the EER spectra related to the optical anisotropy of Cu_2ZnSiS_4 orthorhombic crystal structure. For **E**⊥**c** polarization (Fig. 2(b)), only the feature E_A is seen, while the E_B feature is observed for **E**∥**c** polarization (see Fig. 2(c)). These features may be related to the interband excitonic transitions at the Γ point of the Brillouin zone [18,19]. The EER spectra were analyzed using the first derivative Lorentzian lineshape function model for excitonic transitions [20–22]. This model is given by

$$\frac{\Delta R}{R} = Re\sum_{j=1}^{n} A_j e^{i\phi_j}(E - E_j + i\Gamma_j)^{-2} \quad (1)$$

where n is the number of spectral features to be fitted, A_j and ϕ_j are the amplitude and phase of the lineshape, E_j and Γ_j are, respectively, the energy and broadening parameter of the interband transitions. In Fig. 2 the best least-squares fits to experimental data are shown by the solid curves. Arrows above the curves in Fig. 2 show the positions of the E_A and E_B interband excitonic features. The obtained values of E_A and E_B are found to be 3.345 ± 0.005 eV and 3.432 ± 0.005 eV, respectively, and are listed in Table 1. For comparison purpose, the energy positions determined by PzR [19] are also listed in Table 1. The energy difference between the

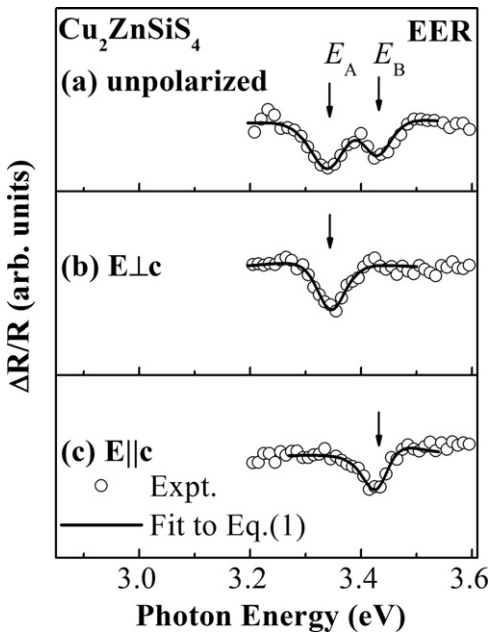

Fig. 2. The (a) unpolarized, (b) **E**⊥**c** polarization and (c) **E**∥**c** polarization EER spectra of Cu_2ZnSiS_4 at 300 K. The solid lines are the least-squares fits of experimental data to Eq. (1). The obtained values of the transition energies denoted as E_A and E_B are indicated by the arrows.

low- and high-energy transitions represents the crystal-field splitting between the two upper-most valence bands. Shay et al. [23] reported the symmetries and splitting of the uppermost valence bands in orthorhombic $AgInS_2$ by using polarized EER measurements on oriented crystals. The observed valence band splitting was explained by crystal field splitting alone, neglecting any spin–orbit interaction. The results showed that the direct band edge transition for **E**∥**c** polarization is higher than that of **E**⊥**c** polarization. Our EER results showed that the excitonic transition energy of E_B feature observed at **E**∥**c** polarization is 87 meV larger than that of E_A at **E**⊥**c** polarization, similar to the deduced value from PzR measurements [19], concurred well qualitatively with the previous report on orthorhombic $AgInS_2$ [23].

Fig. 3(a)–(c) shows the unpolarized, **E**⊥**c** and **E**∥**c** polarization EER spectra of $Cu_2ZnSiSe_4$ in the energy range 2.0–3.0 eV, respectively. As shown in Fig. 3(a), the three dominant structures located between 2.20 and 2.80 eV are associated with band-edge excitonic transitions from different origins and are assigned as E_A, E_B, and E_C. As can be seen in Fig. 3(b), three features are recorded for **E**⊥**c** polarization, whereas in the **E**∥**c** configuration (Fig. 3(c)), only E_B and E_C are the allowed transitions. Shown by the solid curves in Fig. 3(a)–(c) are the least-squares fits to Eq. (1). The dashed curves show the theoretical fit of each transition. Arrows above the curves in Fig. 3 show the positions of the E_A, E_B and E_C interband excitonic features. The obtained values of E_A, E_B and E_C are found to be 2.348 ± 0.005, 2.406 ± 0.005 and 2.605 ± 0.005 eV, respectively, and are listed in Table 1. The observed polarization dependent EER

Table 1
Values of the direct band-edge excitonic transitions E_A, E_B and E_C obtained by fitting EER data to Eq. (1). The corresponding values for the direct excitonic transition energies of Cu_2ZnSiS_4 obtained by piezoreflectance are also listed for comparison.

Materials	Method	E_A (eV)	E_B (eV)	E_C (eV)
Cu_2ZnSiS_4	EER	3.345 ± 0.005	3.432 ± 0.005	–
	PzR[a]	3.323 ± 0.005	3.413 ± 0.005	–
$Cu_2ZnSiSe_4$	EER	2.348 ± 0.005	2.406 ± 0.005	2.605 ± 0.005

[a] Ref. [16].

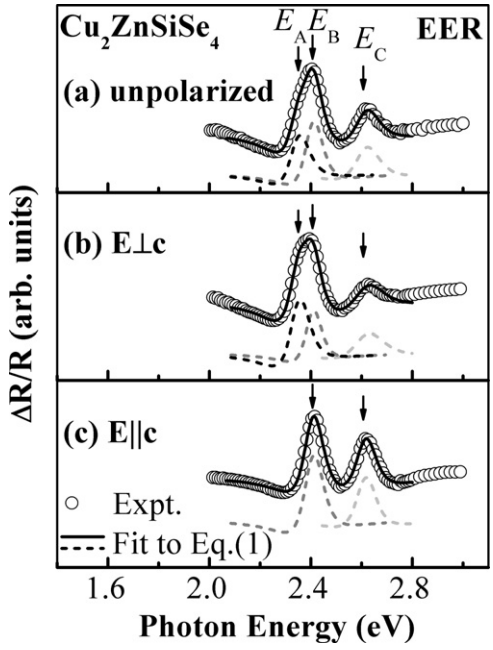

Fig. 3. The (a) unpolarized, (b) **E**⊥**c** polarization and (c) **E**‖**c** polarization EER spectra of $Cu_2ZnSiSe_4$ at 300 K. The solid lines are the least-squares fits of experimental data to Eq. (1). The dashed curves show the theoretical fits to each transition. The obtained values of the transition energies denoted as E_A, E_B and E_C are indicated by the arrows.

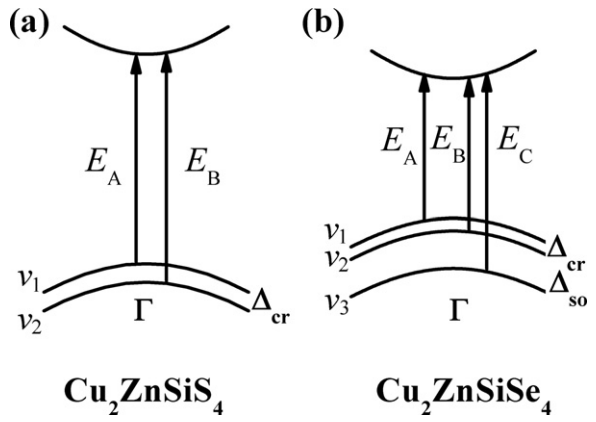

Fig. 4. The schematic representations of the plausible assignments for observed optical transitions near the direct band edge at Γ point for (a) Cu_2ZnSiS_4 and (b) $Cu_2ZnSiSe_4$.

spectra for $Cu_2ZnSiSe_4$ are found to be similar to that reported on photoreflectance (PR) study of wurtzite-CdS by Imada et al. [24]. The results of their polarization dependent PR spectra indicated that as expected from the optical-transition selection rule, the feature E_A can be recognized only for **E**⊥**c**, but not for **E**‖**c**.

Our experimental findings of the near direct band edge transitions for Cu_2ZnSiS_4 and $Cu_2ZnSiSe_4$ are similar to that for I–III–VI_2 semiconductors reported by Shay et al. [25]. They had observed three valence bands in every selenide-containing compound investigated, but never observed three valence bands in a sulphide-based compound. For sulphide contained compounds, only two valence bands were observed, one of which was observed only for **E**⊥**c** and the other for **E**‖**c**. In order to understand the observed interband transitions, a band diagram near the direct band edge is needed. Recently Chen et al. reported a band-structure calculation using first-principles total energy calculations on a family of I_2–II–IV–VI_4 wurtzite-derived polytypes of kesterit and stannite quaternary chalcogenide semiconductors [16,17]. From the calculation, the following results can be found: (i) I_2–II–IV–VI_4 semiconductors have usually direct band gaps at the Γ point, (ii) the top of the valence band is mainly the antibonding component of the p–d hybridization between the group-VI anion and group-I cation, (iii) the bottom conduction band is mainly the antibonding component of the s–s and s–p hybridization between group-IV cation and group-VI anion [17], except for those containing Si, the group-I and group-II cations also have significant contribution to the bottom of the conduction band as well as Si and group-VI anion. Adopting the band-structure calculation by Chen et al. [16] the schematic representation of the plausible assignments for the observed optical transitions near the direct band edge for Cu_2ZnSiS_4 and $Cu_2ZnSiSe_4$ are presented in Fig. 4(a) and (b). As shown in Fig. 4(b), for $Cu_2ZnSiSe_4$ three closely spaced valence bands (ν_1, ν_2 and ν_3) caused by the p–d hybridization of Se p-like and Cu d-like valence band states form the top-most valence bands. We attribute the E_A, E_B, and E_C structures in Fig. 3 to transitions from three split valence bands to a single conduction band minimum at the Γ point, where the differences between ν_1 and ν_2, and ν_2 and ν_3 are the crystal-field (Δ_{cf}) and spin-orbit (Δ_{so}) splitting parameters. For the case of Cu_2ZnSiS_4 $\Delta_{cf} \gg \Delta_{so}$, i.e. spin–orbit splitting can be neglected. Therefore only ν_1 and ν_2 bands form the top-most valence bands (see Fig. 4(a)), and E_A and E_B features in Fig. 2 can be attributed to the transitions from ν_1 and ν_2 to conduction band minimum at the Γ point. Our results also show that the spin split-off energy Δ_{so} in $Cu_2ZnSiSe_4$ is much stronger than that in Cu_2ZnSiS_4 and are attributed to a direct consequence of the heavier Se element. The experimental results agreed well with the recent report by Person [26] on the electronic structure study of Cu_2ZnSnS_4 and $Cu_2ZnSnSe_4$ by a relativistic full-potential linearized augmented plane wave method. The study revealed that the spin split-off energy Δ_{so} is stronger in the Se-based compounds compared to the S-containing compounds.

As shown in Table 1 the crystal field splitting parameter for Cu_2ZnSiS_4 is larger than that of $Cu_2ZnSiSe_4$. The possible reason can be understood as follows. In the simplest approach, the perfect unit cell of orthorhombic $Cu_2ZnSiS_4(Se_4)$ quaternary compounds can be derived by doubling an orthohexagonal wurtzite cell in the a-direction so that the relationship between cells dimensions are $a_{or} = 2a_w$, $b_{or} = \sqrt{3}a_w$, and $c_{or} = c_w$ [2]. In addition, for ideal wurtzite structure, $c_w = 2\sqrt{2/3}a_w$. From the polarized magnetoreflectance measurements on oriented crystals Shih et al. [27] reported that the increase of the crystal-field splitting in $Cu_2Zn_{1-x}Mn_xGeS_4$ is due to the increasing of the fractional distortion from perfect orthorhombic geometry. Using the actual lattice constants of Cu_2ZnSiS_4 and $Cu_2ZnSiSe_4$ [15], the values of the fractional distortion from perfect orthorhombic geometry for a and b axis are −0.0106 and −0.0171 for Cu_2ZnSiS_4 and −0.0085 and −0.0159 for $Cu_2ZnSiSe_4$, respectively. Therefore our experimental finding that the energy difference between the E_B and E_A in Cu_2ZnSiS_4 is higher than that in $Cu_2ZnSiSe_4$ concurred well qualitatively with relative degree of distortion of the respective crystal structures.

4. Summary

Polarization-dependent EER measurements were carried out on the oriented Cu_2ZnSiS_4 and $Cu_2ZnSiSe_4$ single crystals at room temperature. The near direct band edge anisotropic E_A and E_B excitonic transitions of Cu_2ZnSiS_4 are found to be 3.345 eV for **E**⊥**c** and 3.432 eV for **E**‖**c** configurations. For $Cu_2ZnSiSe_4$, three features E_A, E_B, and E_C at around 2.348, 2.406 and 2.605 eV, respectively, were observed for **E**⊥**c** polarization, whereas in the **E**‖**c**, only E_B and E_C were recorded. Based on the experimental results and a recent band-structure calculation by Chen et al., plausible band structures near direct band edge of Cu_2ZnSiS_4 and $Cu_2ZnSiSe_4$ have been presented. The optical transitions are attributed to the transitions from

split valence bands, caused by crystal field and spin orbit interactions, to a single conduction band minimum at the Γ point. Our results reveal that the spin split-off energy Δ_{so} in $Cu_2ZnSiSe_4$ is much stronger than that in Cu_2ZnSiS_4 and are attributed to a direct consequence of the heavier Se element.

Acknowledgments

The authors acknowledge the supports of National Science Council of Taiwan under Project nos. NSC 099-2811-E-011-016, NSC 97-2112-M-011-001-MY3, 98-2221-E-011-015-MY2 and 99-2112-M-032-00-MY3. CHD is thankful to NSRRC for the beam time available on beamlines BL07 and BL12B2.

References

[1] R. Nitsche, D.F. Sargent, P. Wild, J. Cryst. Growth 1 (1967) 52–53.
[2] W. Schafer, R. Nitsche, Mater. Res. Bull. 9 (1974) 645–654.
[3] H. Matsushita, T. Ichikawa, A. Katsui, J. Mater. Sci. 40 (2005) 2003–2005.
[4] O.V. Parasyuk, L.V. Piskach, Y.E. Romanyuk, I.D. Olekseyuk, V.I. Zaremba, V.I. Pekhnyo, J. Alloys Compd. 397 (2005) 85–94.
[5] J.W. Lekse, M.A. Moreau, K.L. McNerny, J. Yeon, P.S. Halasyamani, J.A. Aitken, Inorg. Chem. 48 (2009) 7516–7518.
[6] J.W. Lekse, B.M. Leverett, C.H. Lake, J.A. Aitken, J. Solid State Chem. 181 (2008) 3217–3222.
[7] H. Katagiri, K. Jimbo, S. Yamada, T. Kamimura, W.S. Maw, T. Fukano, T. Ito, T. Motohiro, Appl. Phys. Expr. 1 (2008) 041201 (2pp).
[8] R.A. Wibowo, E.S. Lee, B. Munir, K.H. Kim, Phys. Status Solidi A 204 (2007) 3373–3379.
[9] H. Matsushita, T. Ochiai, A. Katsui, J. Cryst. Growth 275 (2005) e995–e999.
[10] I. Tsuji, Y. Shimodaira, H. Kato, H. Kobayashi, A. Kudo, Chem. Mater. 22 (2010) 1402–1409.
[11] D. Yokoyama, T. Minegishi, K. Jimbo, T. Hisatomi, G. Ma, M. Katayama, J. Kubota, H. Katagiri, K. Domen, Appl. Phys. Expr. 3 (2010) 101202 (3pp).
[12] M.L. Liu, F.Q. Huang, L.D. Chen, I.W. Chen, Appl. Phys. Lett. 94 (2009) 202103 (3pp).
[13] C. Sevik, T. Cagin, Phys. Rev. B 82 (2010) 045202 (7pp).
[14] D.M. Schleich, A. Wold, Mater. Res. Bull. 12 (1977) 111–114.
[15] G.Q. Yao, H.S. Shen, E.D. Honig, R. Kershaw, K. Dwight, A. Wold, Solid State Ionics 24 (1987) 249–252.
[16] S. Chen, X.G. Gong, A. Walsh, S.H. Wei, Phys. Rev. B 79 (2009) 165211 (10pp).
[17] S. Chen, A. Walsh, Y. Luo, J.H. Yang, X.G. Gong, S.H. Wei, Phys. Rev. B 82 (2010) 195203 (8pp).
[18] S. Levcenco, D. Dumcenco, Y.S. Huang, E. Arushanov, V. Tezlevan, K.K. Tiong, C.H. Du, J. Appl. Phys. 108 (2010) 073508 (5pp).
[19] S. Levcenco, D. Dumcenco, Y.S. Huang, E. Arushanov, V. Tezlevan, K.K. Tiong, C.H. Du, J. Alloys Compd. 506 (2010) 46–50.
[20] F.H. Pollak, H. Shen, Mater. Sci. Eng. R 10 (1993), xv–xvi.
[21] Y.S. Huang, F.H. Pollak, Phys. Status Solidi A 202 (2005) 1193–1207.
[22] D.E. Aspnes, in: T.S. Moss, M. Balkanski (Eds.), Handbook of Semiconductors, vol. 2, North-Holland, Amsterdam, 1980, pp. 109–154.
[23] J.L. Shay, B. Tell, L.M. Schiavone, H.M. Kasper, F. Thiel, Phys. Rev. B 9 (1974) 1719–1723.
[24] A. Imada, S. Ozaki, S. Adachi, J. Appl. Phys. 92 (2002) 1793–1798.
[25] J.L. Shay, B. Tell, H.M. Kasper, L.M. Schiavone, Phys. Rev. B 5 (1972) 5003–5005.
[26] C. Person, J. Appl. Phys. 107 (2010) 053710 (8pp).
[27] O.W. Shih, R.L. Aggarwal, T.Q. Vu, Y. Shapira, K. Doverspike, R.N. Kershaw, K. Dwight, A. Wold, Phys. Rev. B 45 (1992) 14025–14035.